MECHANICS OF ADVANCED MATERIALS AND STRUCTURES
2018, VOL. 0, NO. 0, 1–9
https://doi.org/10.1080/15376494.2018.1475584

Taylor & Francis
Taylor & Francis Group

ORIGINAL ARTICLE

Dynamic strain rate and relative density effect on compression behavior of PP and PP/PE copolymers foamed by microcellular injection molding

T. Gómez del Río[a], J. Rodriguez[a], D. Arencón[b], and A. B. Martínez[b]

[a]Grupo de Durabilidad e Integridad Mecánica de Materiales (DIMME), Universidad Rey Juan Carlos, Madrid, Spain; [b]Department of Materials Science and Metallurgy, Centre Català del Plàstic, Universitat Politècnica de Catalunya – Barcelona TECH, Terrassa, Spain

ABSTRACT

Isotactic polypropylene–polyethylene copolymer microcellular foams of various relative densities were prepared using nitrogen (N_2) in supercritical solid state. Also, series of copolymers with different polyethylene weight percentages were prepared. Mechanical properties (compression and impact conditions) dependence on relative density, PE content, and strain rate was studied. Results showed that yield stress gradually decreased with lower density. The yield stress of PP copolymer foams decreased with the relative densities, and was always smaller than that of the solid PP copolymer. Nevertheless, the sensibility to strain rate effect decreases at impact velocities. Analytical models were developed including the effects of both relative density and strain rate.

ARTICLE HISTORY
Received 7 May 2018
Accepted 8 May 2018

KEYWORDS
Microcellular foam; mechanical properties; strain rate; relative density

1. Introduction

The mechanical properties of cellular foams with densities around 10 times less compared to the density of the solid polymer have been extensively investigated [1]–[5]. It was shown that the properties such as strength-to-weight ratio of these foams are significantly improved, but it has been observed that a decrease in cell size would achieve even greater improvement in these properties. Thus was born the idea of manufacturing foams with cell sizes of microns, i.e., microcellular foams [6]–[8], or even nano, i.e., nanocellular foams, with densities around 80% and 90% less than the solid polymer density [9]–[10], which have been probed to have a good strength and fracture behavior for the intended applications.

Since 1990s, the new concept of microfoam was developed: by reducing the cell size to 10 μm or even less, microcellular foams can reduce significantly the amount of plastics used while improving some mechanical properties, and may offer special properties that are not possessed by the cellular foams or the solid polymers. Microcellular foams have average cell sizes in the order of 10–100 μm. So, they show cell densities around 10^9 cells/cm^3 [8]. Compared to un-foamed polymers and conventional foams, microcellular foams have shown superior mechanical properties such as high impact strength [11]–[13]; high toughness [14], high stiffness-to-weight ratio [15], high fatigue life [16], and reduced material weight and cost.

Mechanical properties of microcellular foams have been investigated previously. And, unlike conventional foams, they exhibit consistent and improved mechanical properties in different polymers in systems such as polycarbonate (PC), polyethylene terephthalate (PET), poly(vinyl chloride) (PVC), or acrylonitrile butadiene styrene (ABS) [17]. For example, yield stress has been modeled to vary linearly with the relative density of the foam [18], [19]. It has been assumed that the reason of this improvement is the reduction of cell size as well as the uniform and homogeneous cell structure of microcellular foams. Gibson and Ashby developed models for mechanical properties, such as Young's modulus and strength, which show the dependence between density and physical properties of the cellular materials [18].

MuCell® technology is based on the direct injection of atmospheric gas (N_2, CO_2) in its supercritical state. Injection during the supercritical state allows for a single phase gas/polymer solution. This injection molding technology (Trexel Inc., MA, USA) can be used with thermoplastics materials. With this technique, the material is lighten and provides foams with unique flexibility and cost savings as it uses less material, cycle time, processing temperature, and clamping force. The MuCell® process allows for plastic part design optimized for functionality. The combination of density reduction and design for functionality often results in material and weight savings. The influence of the processing parameters on cell structure and mechanical properties has been investigated in a wide range of plastics (PP, PET, PA6, PC, LDPE, and ABS), and in some of their reinforced composites with glass fiber or nanoclay particles [20].

There are many research papers on theoretical and experimental studies comparing mechanical properties of conventional polymers with their microcellular foams [21]–[23], at a low loading rate or under quasi-static conditions. As these materials are used in many applications as energy absorbers in impacts, the knowledge of their properties at high strain rates is

CONTACT Teresa Gómez del Río mariateresa.gomez@urjc.es Grupo de Durabilidad e Integridad Mecánica de Materiales (DIMME), Universidad Rey Juan Carlos, C/Tulipán s/n, 28933 Madrid, Spain.
Color versions of one or more of the figures in the article can be found online at www.tandfonline.com/umcm.

crucial. Even more, it should be very helpful having equations of yield stress or Young's modulus depending on both high strain rate and relative density. But, as far as the authors' knowledge, there are very few works that have studied the high strain rate mechanical properties of microcellular foams. Nevertheless, it is obvious that, in order to optimize the design of structures used against impacts, it is necessary to study and understand the response of these materials under actual working and service conditions. The strain rate sensitivity of polymers is expected due to the viscoelasticity of the material.

Due to its good ductility and stiffness, moisture, and chemical resistance, PP is one of the most common polymers used. It is also easily processed, versatile, and has a low cost. Nevertheless, PP shows very low impact strength so its use is limited in structural applications. One of the solutions to this problem has been the addition of a second rubbery phase. Modified polypropylenes with different impact modifiers have been studied: for example, blends of propylene–ethylene–diene terpolymer (EPDM) and polypropylene, ethylene/propylene block copolymers (EPR), and styrene–ethylene/1-butene–styrene block copolymers (SEBS). Although a variety of elastomers have been studied, the two first mentioned are the most commercialized due to the low cost of processing [23].

In the present work, one polypropylene and four ethylene/propylene block copolymers were used to inject cylindrical bars, obtaining solid and foamed specimens. By varying the gas content, different levels of foaming and relative density were achieved. Mechanical properties were determined through compression tests at different strain rates (10^{-3}–3×10^{3} s^{-1}) using a universal testing machine and a Hopkinson bar device. Yield stress gradually decreased with decreasing apparent density. New equations that content the dependence with both strain rate and relative density together have been developed. Experimental results were related to relative density, and prediction models were employed to compare the estimated values to the experimental data.

2. Experimental procedure

2.1. Material and specimens

This work deals with five different polymers: one polypropylene homopolymer (PP) and four ethylene/propylene block copolymers with diverse percentage of polyethylene (BC1, BC5, BC7, and BC8). Properties of these five polymers are presented in Table 1.

2.2. Foaming procedure

In this work, injection molding was used to obtain the samples. The machine selected for the manufacturing process was a Victory 110 (Engel GmbH) equipped with a MuCell® package containing a special plasticizing unit with a 40-mm screw and maximum swept volume of 251 cm^3 and one supercritical fluid (SCF) series II 25-mm injection valve. Also, for the production of the foamed parts, an MTR-3 mold temperature controlling device was added. Finally, the whole manufacturing system includes an SCF SII delivery system and piping, as well as instrumentation. The physical foaming agent employed was N_2.

The injection temperature profile employed was constant: 190–230°C, with increments of 10°C from hopper to nozzle, and mold temperature was set at 40°C. The injection speed was 130 cm^3/s, and the N_2 flow rate was varied to obtain the desired foaming grade. Melt plasticizing pressure was monitored to range at 198 atm and the cooling cycle was kept constant at 30s. The injection-molded samples according to all these conditions were cylindrical bars, each having a diameter of 8 mm.

Table 1. Basic properties of the solid copolymers under study.

Sample	Ethylene (wt%)	Isotacticity (%)	Mn (kg/mol)
PP	0	90	126
BC1	6.9	89.3	160.5
BC5	8.5	85.4	65.7
BC7	8.5	84.2	56.1
BC8	11.2	81	60.8

2.3. Thermal, morphological, and physico-chemical characterization

Dynamic mechanical properties were determined with a TA Instrument DMTA Q800 operating in single cantilever mode with three oscillation frequencies. The glass transition temperature was measured with this equipment. The crystallinity index, λ, of the two samples was measured via differential scanning calorimetry (DSC) using a Mettler Toledo (model DSC822) equipment. Samples were extracted from several sections of the injected bars. Heating scans were performed from 40 to 200 °C at 10 °C/min. All runs were carried out in a stream of dried nitrogen. The crystallinity index (λ) is calculated according to the following equation:

$$\lambda = \frac{\Delta H_f}{\Delta H_0^{PP} f^{PP} + \Delta H_0^{PE} f^{PE}} \quad (1)$$

where ΔH_f represents the fusion enthalpy, ΔH_0^{PP} and ΔH_0^{PE} represent the ideal fusion enthalpy of 100% crystalline PP and PE, respectively, and f^{PP} and f^{PE} the corresponding fractions (%). The theoretical values taken from previous works [5] were 207 and 296 J/g, respectively. was the melting enthalpy measured in the heating or cooling experiments, and ΔH_0 is the theoretical enthalpy of PP 100% crystalline ($\Delta H_0 = 207.1$ J/g). Q1

X-ray diffraction (XRD) of the samples was measured with an X'Pert PRO diffractometer from Panalytical using a Cu Kα ($\lambda = 1.5406$ Å) radiation source operated at a voltage of 45 kV and electric current of 300 mA. The 2θ scanning range was 10–80°.

A Mettler Toledo balance, with ±0.001 mg, equipped with a density determination kit by means of the buoyancy technique, was used to measure the density of the injected solid and foamed polymers. Three specimens were measured for each kind of foam, and also each specimen was measured at least five times for determining an average value.

2.4 Compression tests

In order to measure the influence of strain rate on the mechanical properties of microcellular polypropylenes, compression tests have been performed in the range of strain rates: from quasi-static (10^{-3} s^{-1}) to impact (3×10^{3} s^{-1}) velocities.

The device selected for the quasi-static tests was an electromechanical MTS universal testing machine. This machine is equipped with a load frame of 100 kN, so a smaller one was added in this work, a 5 kN load frame, in order to have a better resolution in the force data recording. Three different engineering strain rates (10^{-3}, 10^{-2}, and 10^{-1} s^{-1}) were selected to study the effect of strain rate in quasi-static compression tests. The samples used were cylinders 12 mm in height and 8 mm in diameter machined from the previous injection-molded bars. In order to minimize interfacial friction, all specimens were lubricated. Between three and five specimens were tested for each material and velocity, for evaluation of the test reproducibility.

The displacement and strain fields of each specimen tested were analyzed using a LIMESS video-extensometer. The yield stress was obtained from the loading history.

Impact tests were performed with a common Split Hopkinson pressure bar (SHPB). This device is extensively described in a previous paper [25]. Polymer materials show a small impedance ($Z = \rho c$) compared to that of the device bars, approximately 40 times higher than that of the microcellular foams used. Nevertheless, the tests results show that the impedance mismatch was acceptable.

The sample dimensions in SHPB tests need to meet some conditions. The stress equilibrium must be achieved during the whole test and the specimen should be long enough to assure the friction effect can be neglected and behave as the massive material. So, the length to diameter ratio must be chosen.

According to previous works, the equilibrium is achieved after approximately four wave reverberations in the specimen, so an initial period that has to be as short as possible is needed, and this period is dependent on the wave velocity within the specimen. The final solution was reducing, not much according to the other friction condition, the thickness of the specimen compared to the high as that of quasi-static test samples. As for the behavior of the massive material, due to the size of the bubbles and the microstructure of the microcellular foams, small specimens can be enough representatives. Finally, a thickness of 3 mm was used. Moreover, some specimens of 3 mm height were tested under quasi-static conditions to verify there was no effect of the specimen size. Stress-strain curves for the various relative density foams are plotted in Figure 1.

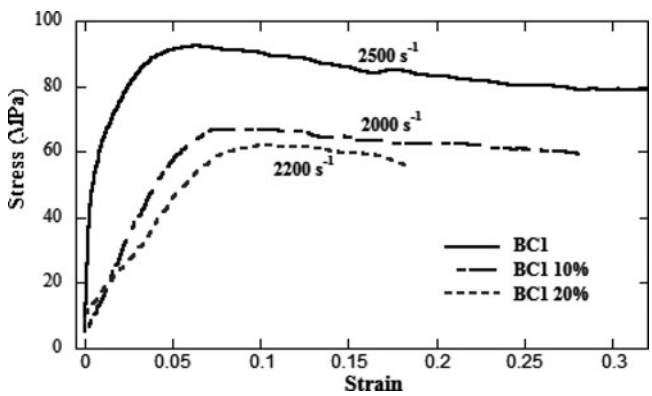

Figure 1. Stress-strain curves of the BC1 copolymer microcellular foams at high strain rate compression loading.

Table 2. Thermal and morphological parameters from DMTA, DSC, and XDR measurements.

	DMTA		DSC (crystalline index, %)		XDR
	T_g PP (°C)	T_g PE (°C)	λ PP	λ PE	χ_c(%)
PP	12	—	47.3	—	54.7
BC1	10.6	− 45.8	41.6	0.19	59
BC5	10.4	− 49.3	44.6	0.23	63
BC7	10.5	− 49.4	45.3	0.21	61
BC8	11.7	− 48.5	46.2	0.42	60

3. Results and discussion

3.1. *Density, thermal, and morphological characterization*

Table 2 presents the data obtained from the DSC, DMTA, and XRD measurements. The block copolymers present two values of these properties: first corresponding to propylene and second to polyethylene.

The foaming grade is usually explained in terms of relative density of the foams, i.e., the ratio of the foam density to the solid polymer density. Table 3 shows the mean values of the test performed for the solid PP and copolymers, compared to their microcellular foams.

3.2. *Mechanical results*

The mechanical behavior of the microcellular foams studied is shown in the true stress-true strain curves in Figures 1 and 2 As polymers undergo large deformation, true stress ($\sigma = \frac{F}{S}$, considering the variation of section) and true strain, $\varepsilon = \ln(1 + \Delta l/l_0)$, are more appropriate to show the mechanical behavior of the samples tested. For the sake of clarity, in Figures 1 and 2, only results from one test, for one copolymer (BC1) and one strain rate (2×10^3 and 10^{-2} s^{-1}, respectively), are plotted.

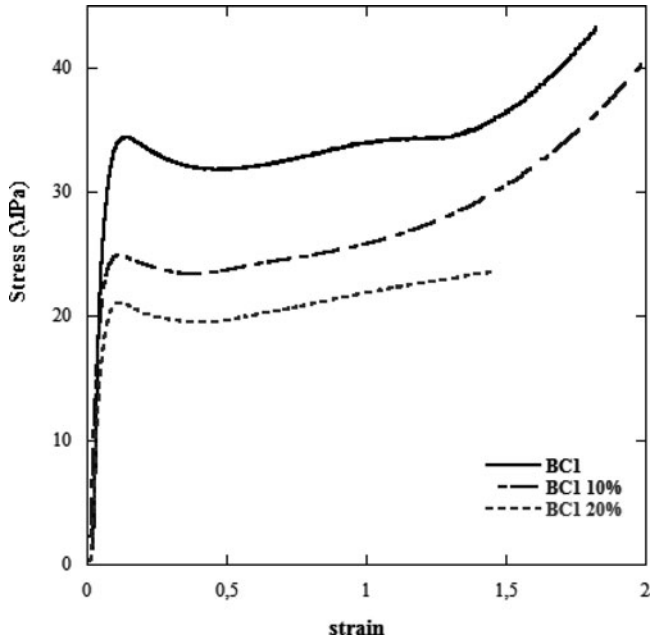

Figure 2. Stress-strain compression loading curves of the BC1 copolymer microcellular foams at 10^{-2} s^{-1}.

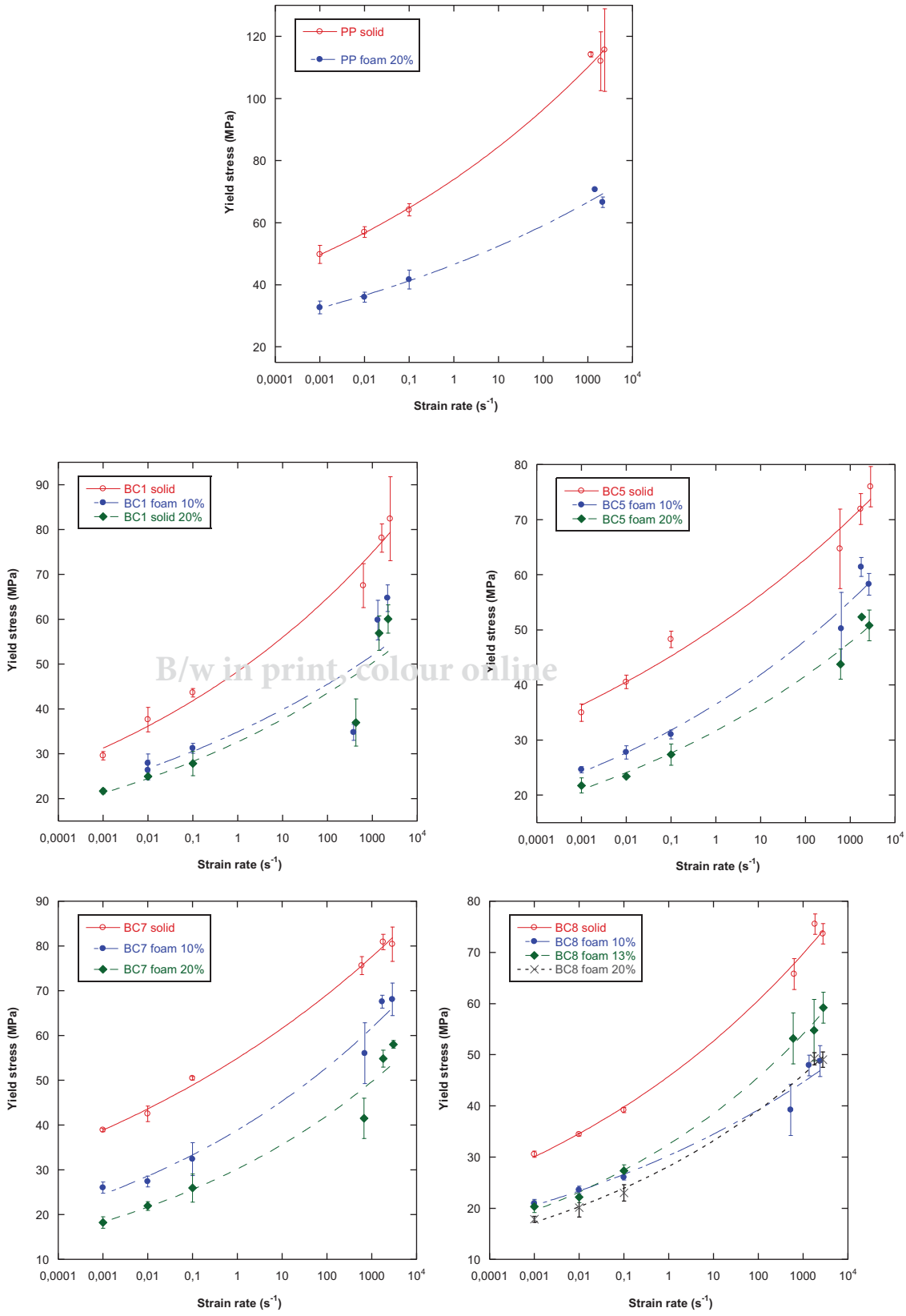

Figure 3. Yield stress vs. strain rate for all the microcellular foams for each relative density and material tested: PP homopolymer and copolymers BC1, BC5, BC7, and BC8. Experimental values are plotted as points and the lines are representing the fitted model.

Table 3. Densities and foaming grade of samples studied.

Material	PP		BC1			BC5			BC7			BC8			
Foaming grade (%)	0	20	0	10	20	0	10	20	0	10	20	0	10	13	20
Density (g/cm^3)	0.881	0.751	0.885	0.763	0.682	0.883	0.786	0.716	0.885	0.773	0.721	0.891	0.798	0.768	0.691

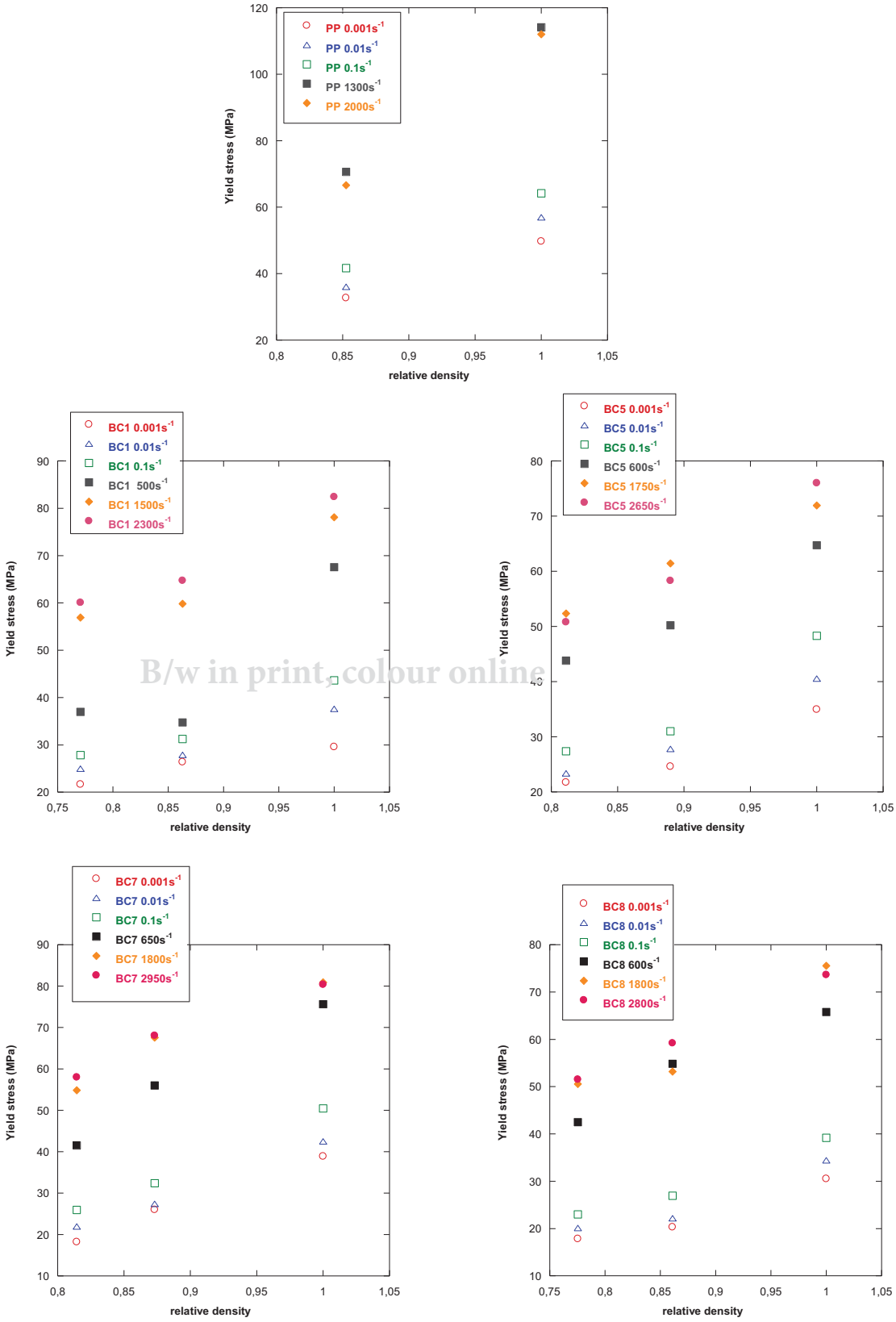

Figure 4. Yield stress vs. relative density at different strain rates (both high and low strain rates) for the PP homopolymer and for each copolymer (BC1, BC5, BC7, and BC8).

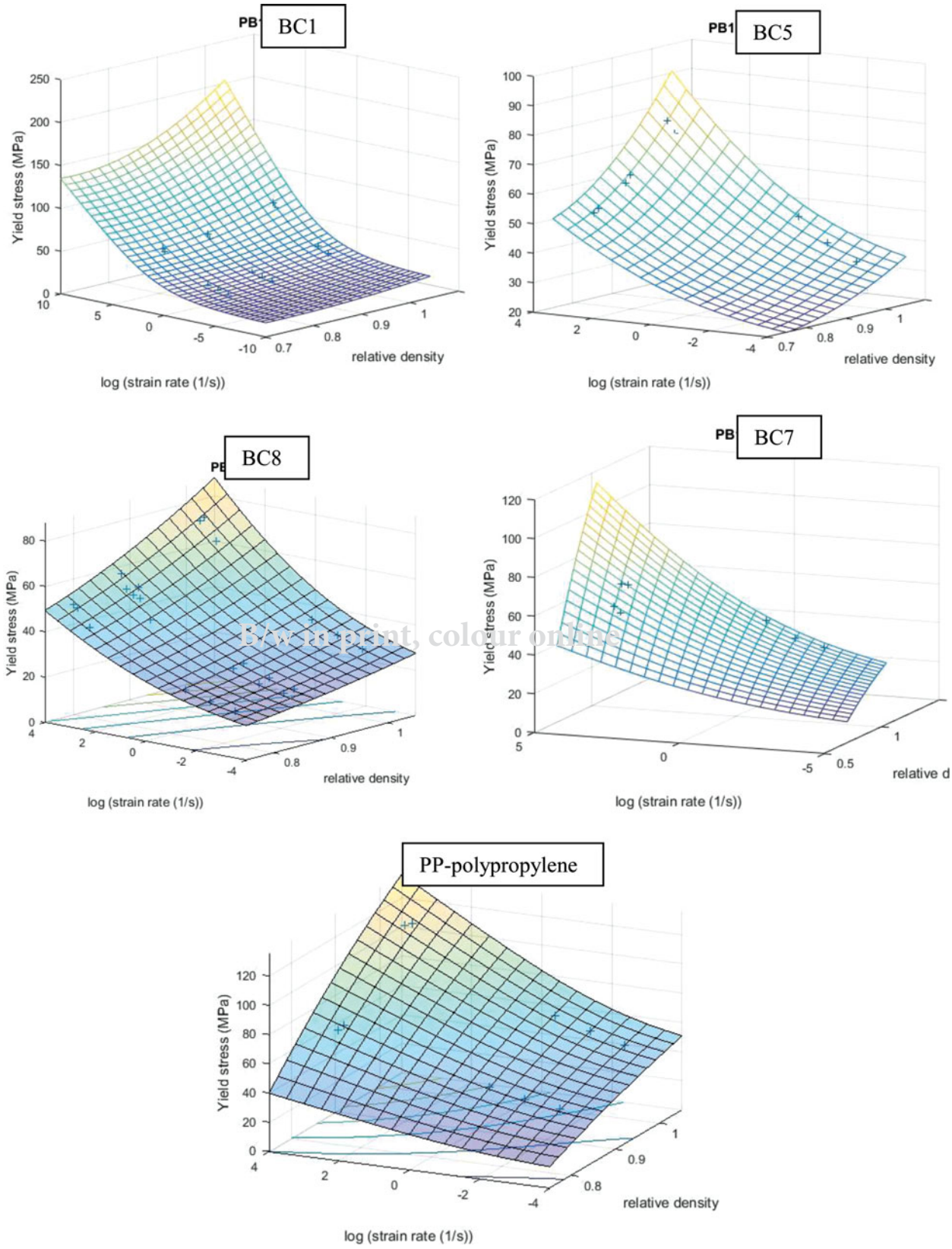

Figure 5. Fitting surfaces of yield stress considered as function of relative density and strain rate (Eq. (7)) for the PP homopolymer and the four copolymers studied. Experimental values are plotted as crosses.

The mechanical behavior of these foams at quasi-static compression can be divided in three main parts: first, a linear elastic behavior ended in a soft peak of stress. This maximum is considered as the start of the plastic zone, i.e., the reach of yield stress. A second part with a negative slope and nonlinear regression is considered as softening (3), and third, a long stage of small stress increment, or even constant stress stage, which consists of foam densification.

In order to obtain the stress-strain curves for impact rates of strain, the Hopkinson bar is instrumented with strain gauges bonded to the incident and transmitted bars. These gauges provide strain pulses as output. The strain rate, stress, and strain are calculated, once the equilibrium is reached, from the strain pulses by the following equations:

$$\dot{\varepsilon}(t) = \frac{2c_b\varepsilon_r(t)}{l_0} \tag{2}$$

$$\varepsilon(t) = \int_0^t \dot{\varepsilon}(\tau)\, d\tau \tag{3}$$

$$\sigma(t) = \frac{A\varepsilon_t(t)}{A_0} E_b \tag{4}$$

where $\varepsilon_r(t)$ and $\varepsilon_t(t)$ are the reflected and transmitted strain pulses registered in the strain gauges, respectively, over time t, and τ is a time variable used for integration. E_b, c_b, and A are the Young's modulus, sound wave velocity, and cross-sectional area and of the device steel bars, respectively. For the specimen, l_0 and A_0 are the length and cross-sectional area, respectively.

The trend observed in stress-strain graphs in Figure 1 and 2 is typical of foams and other porous materials, where a zone of constant stress, or small increase, is observed after the linear region and the reach of yield stress. This zone corresponds to plastic deformation of cell walls and compaction of porosity by the compressing material. At the end of the plateau region, the foam densification completes and the stress increases [22]. The stress-strain graphs for quasi-static and high strain rate compression for all five types of foams show a similar trend. No fracture point is seen in the specimens tested even after 90% strain.

In order to assess the effect of relative density and strain rate on the compression behavior of the microcellular foams studied, a parameter must be chosen. In this work, the yield stress (as defined previously) has been identified as the more representative of the mechanical behavior as it means the onset of plastic and plateau zones of the materials.

Figure 3 shows curves of yield stress versus strain rate. Five graphs are displayed, so each material is compared with its different relative density foams. An increase in strength with the strain rate can be appreciated not only for the solid polymer but also for the foams. Nevertheless, this increment is smaller as the density decreases: denser foams seem to be more influenced than the lowest density foams.

It is well known that polymers exhibit a viscoelastic behavior. In these materials, the plastic deformation is identified as a thermally activated process due to the movement of chains of molecules. Based on this fact, the strain rate dependency of yield stress has been successfully described by the Ree–Eyring model [26]. This previous model was not able to describe the dependence at very high strain rates, and a new model was proposed by Fotheringham and Cherry [27]. It introduced the idea that yielding needs the cooperative motion of multiple chain segments and an internal stress as a new structural parameter. In previous works [25], [28], the authors have studied the strain rate dependence of some polymers and made a brief review of the different models found in the literature; the dependence of yield stress on strain rate and temperature for this kind of polymers is well described by the following expression [29]:

$$\sigma_y = \sigma_i(0) - mT + \frac{2kT}{V}\sinh^{-1}\left[\frac{\dot{\varepsilon}}{\dot{\varepsilon}_0 \exp\left(-\frac{\Delta H}{kT}\right)}\right]^{1/n} \tag{5}$$

$$\sigma_y = \sigma_i(0) - mT + \frac{2kT}{V}\sinh^{-1}\left[\frac{\dot{\varepsilon}}{\dot{\varepsilon}^*(T)}\right]^{1/n} \tag{6}$$

where σ_y is the yield stress, $\sigma_i(T)$ is the constant value of stress for each material, T is the absolute temperature, k is Boltzmann's constant, $\dot{\varepsilon}^*(T)$ is the reference strain rate, ΔH and V are the activation energy and activation volume, respectively, and n is a material parameter used to characterize the cooperative movement of chain segments.

Figure 4 shows yield stress, σ_y, as a function of foam density in all the strain rate range tested, for each kind of polymer: PP, BC1, BC5, BC7, and BC8. Cellular solid properties depend on both the topology and material. The properties of the solid of which the foam is made and the topology and shape of the cells edges and faces and so, the relative density, $(\frac{\rho}{\rho^*})$, of the foam, where ρ is the density of the foam and ρ^* that of the solid of which it is made.

According to Gibson and Ashby [18], [19], [30], the yield stress in foams with regular cell microstructure will follow an equation like

$$\frac{\sigma_{y\_foam}}{\sigma^*_{y\_solid}} = 0.3\left(\varphi\frac{\rho}{\rho^*}\right)^{3/2} + 0.4(1-\varphi)\left(\frac{\rho}{\rho^*}\right) + \frac{p_0 - p_{atm}}{\sigma^*_{y\_solid}} \tag{6}$$

where σ_{y_foam} is the yield stress of the foam, $\sigma^*_{y\_solid}$ is the collapse stress of the solid material, φ is the relative volume of the faces to the edges in the closed-cell foams, p_0 is the fluid pressure in closed-cell foam cells, and p_{atm} is the atmospheric pressure. This equation is based on a micromechanical model that considers the deformation mechanisms of the microcell structure under loading [6]. It is based on regular structures with the same proportion of walls and edges for all the cells, and also similar size. The first term in the equation is due to the bending dominant behavior of the walls in the cells and the linear term refers to the plastic stretch dominated failure in the struts. Ma et al. [31] verified that microcellular foams with an irregular distribution of cell sizes would not follow the Ashby and Gibson law, as the cell size distribution will have an effect on the yield stress. Finally, they propose the following equation:

$$\frac{\sigma_{y\_foam}}{\sigma^*_{y\_solid}} = C_1\left(\lambda\phi\frac{\rho}{\rho^*}\right)^2 + C_2\left(\lambda\phi\frac{\rho}{\rho^*}\right)^{3/2} + C_3\left(\lambda\phi\frac{\rho}{\rho^*}\right) + C_4 \tag{7}$$

where λ is the distribution coefficient that takes into account the cell size distribution, and C_1, C_2, C_3, and C_4 are parameters obtained by the best fitting of the experimental values.

Table 4. Values of the parameters required by the models.

Parameter	PP	BC1	BC5	BC7	BC8
A_1	10.44	−10.9	−10.47	7.5	−2.975
A_2	−5.482	8.5	8.55	−3.9	2.887
A_3	−3.94	3.3	2.92	−2.6	0.7872
N	5.41	7.35	8.00	9.90	8.69
V_{eff} (nm^3)	0.2790	0.1350	0.1925	0.1305	0.1126
$\sigma_i^*(T)$ (MPa)	36.43	25.00	24.95	18.10	21.06
$\dot{\varepsilon}^*(T)$ (s^{-1})	0.07	315	115	114.5	100.2

Based on both Ma et al. and Gibson and Ashby models, a simply new equation was proposed considering only the powers of $\frac{\rho}{\rho^*}$ affecting the yield stress according to Gibson and Ashby, which are equal to 1 and 3/2, and the inner fluid but letting the coefficients of the model to fit freely the experimental values:

$$\frac{\sigma_{y\_foam}}{\sigma^*_{y\_solid}} = A_1\left(\frac{\rho}{\rho^*}\right) + A_2\left(\frac{\rho}{\rho^*}\right)^{3/2} + A_3 \tag{8}$$

where A_1 and A_2 are parameters associated not only with the geometrical morphology but also the failure mode in the cells; moreover, these parameters are related to closed-cell foams but with cells of nonregular shape and size. Microcellular foams made by injection molding with supercritical gas usually show a nonregular distribution of the size of cells and a solid skin. In this new equation, A_1 and A_2 are the parameters that take into account this effect, and A_3 is the parameter that refers to the pressure of the fluid inside the cells. The linear term stands for the buckling of the cell edges and the power term describes the proportion of wall collapse.

Combining Eqs. (4) and (7), the yield stress of the polymer foams can be expressed only in terms of its relative density and the strain rate as independent variables

$$\sigma_{y\_foam} = \left[A_1\left(\frac{\rho}{\rho^*}\right) + A_2\left(\frac{\rho}{\rho^*}\right)^{3/2} + A_3\right] \times \left[\sigma_y^*(T) + \frac{2kT}{V_{eff}}\sinh^{-1}\left[\frac{\dot{\varepsilon}}{\dot{\varepsilon}^*(T)}\right]^{1/n}\right] \tag{9}$$

where $\sigma_i^*(T)$ and $\dot{\varepsilon}^*(T)$ are constants, which show the properties of the solid material at the test temperature. Experimental data were fitted to Eq. (7) using all the yield data at once. Table 4 shows the model parameters obtained for the materials under study, and the surface fitting is shown in Figure 5. Regression parameters are above 0.97 in all cases studied. The model parameters were obtained for all materials under study: PP, BC1, BC5, BC7, and BC8. They are in the same order of magnitude than those found in bibliography for other polypropylenes and block propylene/ethylene copolymers [25, 28]. The parameter n is related to the number of segments involved in the plastic deformation. Previous works suggested that higher crystalline percentage implies more cooperative segmental motion [6], and this agrees with the smaller value of n for the copolymers. The activation volume, V_{eff}, is in the order of 10^{-28} m^3; the same order as the previous work [28] for activation volumes were calculated using the Richeton and Eyring model. The preexponential strain rate is roughly in the same order of magnitude as the Debye frequency (10^{14}–10^{17} Hz). The activation energy, ΔH_{eff}, is in the same range as those obtained for the β activation energy [28]. The values are also in the same order of those obtained by Vu-Khanh and El Majdoubi [32] for polypropylenes with different crystalline percentages. The values of the parameter $\sigma_i^*(T)$ are consistent with the relationship predicted by Rault [33] for semi-crystalline polymers at room temperature.

4. Conclusions

In this work, the dependence of yield stress of microcellular foam polymers on relative density and strain rate has been studied. It is important to point out that the dependence of both variables has been modeled together.

Different polymers were selected to manufacture microcellular foams. All the polymers were based on polypropylene, and the difference in the solid samples was the percentage of polyethylene.

Then, between two and four foams of different grades were manufactured by microcellular injection molding. After testing five different copolymers under uniaxial compression loading, with relative densities between 0.8 and 1, in the range 10^{-3}–3×10^3 s^{-1}, the experimental results provides the following conclusions:

Polypropylene homopolymer and the four ethylene/propylene block copolymers were studied and their microcellular foams show a significant increase of compression yield stress with strain rates and relative density. The dependence on relative density has been modeled as polynomial and the effect of strain rate goes with the inverse hyperbolic sine. This model captures the huge increase accentuated at very high rates of strain, such as those characteristic of Hopkinson Bar experiments. Nevertheless, the compression yield stresses of the ethylene/propylene block copolymers are always lower than the polypropylene homopolymer values.

Another conclusion based on the experimental results of this work is related with strain rate sensitivity. It could be expected that the foam yield stress increases with the relative density, but based on the results of this work, it can be concluded that the strain rate sensitivity (increase in the yield stress) is less pronounced in foamed polymers compared to the solid ones.

Finally, a constitutive equation has been proposed for the microcellular foams. This equation has taken into account both the strain rate effect and the relative density effect in a mechanical property of polymers such as yield stress. The new model proposed fits the experimental data regression parameters above 0.97 in all cases studied.

References

[1] L. J. Gibson and M. F. Ashby, *Cellular Solids: Structure and Properties*. Cambridge: Cambridge University Press, 1997.

[2] R. Bouix, P. Viot, and J. L. Lataillade, "Polypropylene foam behaviour under dynamic loadings: Strain rate, density and microstructure effects," *Int. J. Impact Eng.*, vol. 36, pp. 329–342, 2009. DOI: 10.1016/j.ijimpeng.2007.11.007.

[3] P. Viot, F. Beani, and J. L. Lataillade, "Polymeric foam behaviour under dynamic compressive loading," *J. Mater. Sci.*, vol. 40, pp. 5829–5837, 2005. DOI: 10.1007/s10853-005-4998-5.

[4] J.-J. Hwang, T. Adachi, T. Kuwabara, and W. Araki, "Laminate model expressing mechanical properties of polypropylene foams having

non-uniform cell-shape distributions," *Mater. Sci. Eng. A*, vol. 487, pp. 369–376, 2008. DOI: 10.1016/j.msea.2007.10.060.

[5] D. Arencón, M. Antunes, A. B. Martínez, and J. I. Velasco, "Study of the fracture behaviour of flexible polypropylene foams using the essential work of fracture (EWF)," *Polym. Testing*, vol. 31, pp. 217–225, 2012. DOI: 10.1016/j.polymertesting.2011.10.013.

[6] D. Miller and V. Kumar, "Microcellular and nanocellular solid-state polyetherimide (PEI) foams using sub-critical carbon dioxide II. Tensile and impact properties," *Polymer*, vol. 52, no. 13, pp. 2910–2919, 2011.

[7] B. Notario, J. Pinto, and M. A. Rodríguez-Pérez, "Nanoporous polymeric materials: A new class of materials with enhanced properties," *Progress Mater. Sci.*, vol. 78–79, pp. 93–139, 2016. DOI: 10.1016/j.pmatsci.2016.02.002.

[8] V. Kumar, M. VanderWel, J. Weller, and K. A. Seeler, "Experimental characterization of the tensile behavior of microcellular polycarbonate foams," *J. Eng. Mater. Technol.*, vol. 116, no. 4, pp. 439–445, 1994. DOI: 10.1115/1.2904310.

[9] J. Li et al., "Preparation and mechanical properties of thermosetting epoxy foams based on epoxy/2-ethyl-4-methylimidazol system with different curing agent contents," *J. Cell. Plast.*, vol. 53, no. 6, pp. 663–681, 2017. DOI: 10.1177/0021955X17695095.

[10] T. Liu, H. Liu, L. Li, and X. Wang, "Microstructure and properties of microcellular poly (phenylene sulfide) foams by MuCell injection molding," *Polym.–Plast. Technol. Eng.*, vol. 52, no. 5, pp. 440–445, 2013. DOI: 10.1080/03602559.2012.748803.

[11] E. Laguna-Gutierrez, R. Van Hooghten, P. Moldenaers, and M. A. Rodríguez-Pérez, "Understanding the foamability and mechanical properties of foamed polypropylene blends by using extensional rheology," *J. Appl. Polym. Sci.*, vol. 132, no. 33, pp. 42430–4243, 2015. DOI: 10.1002/app.42430.

[12] L. M. Matuana, C. B. Park, and J. J. Balatinecz, "Structures and mechanical properties of microcellular foamed polyvinyl chloride," *Cell. Polym.*, vol. 17, no. 1, pp. 1–16, 1998.

[13] D. I. Collias, D. G. Baird, and R. J. M. Borggreve, "Impact toughening of polycarbonate by microcellular foaming," *Polymer*, vol. 35, no. 18, pp. 3978–3983, 1994. DOI: 10.1016/0032-3861(94)90283-6.

[14] D. F. Baldwin and N. P. Suh, "Microcellular Poly (ethylene terephthalate) and crystallisable poly (ethylene terephthalate): Characterization of process variables," in *Proc. ANTEC '92, SPE Tech. Paper*, vol. 38, 1992, pp. 1503–1507.

[15] D. Klempner and K. C. Frisch, *Handbook of Polymeric Foams and Foam Technology*. Munich: Hanser Publishers, 1991.

[16] K. A. Seeler and V. Kumar, "Tension-tension fatigue of microcellular polycarbonate: Initial results," *J. Reinf. Plast. Compos.*, vol. 12, no. 3, pp. 359–376, 1993. DOI: 10.1177/073168449301200308.

[17] C. Jo, J. Fu, and H. E. Naguib, "Constitutive modelling for mechanical behaviour of PMMA microcellular foams," *Polymer*, vol. 46, no. 25, pp. 11896–11903, 2005. DOI: 10.1016/j.polymer.2005.09.054.

[18] L. J. Gibson and M. F. Ashby, "The mechanics of three-dimensional cellular materials," *Proc. R. Soc. Lond. Ser. A, Math. Phys. Sci.*, vol. 382, no. 1782, pp. 43–59, 1982. DOI: 10.1098/rspa.1982.0088.

[19] L. J. Gibson, M. F. Ashby, G. S. Schajer, and C. I. Robertson, "The mechanics of two-dimensional cellular materials," *Proc. R. Soc. Lond. Ser. A, Math. Phys. Sci.*, vol. 382, no. 1782, pp. 25–42, 1982. DOI: 10.1098/rspa.1982.0087.

[20] J. Gómez-Monterde et al., "Morphology and mechanical characterization of ABS foamed by microcellular injection molding," *Proc. Eng.*, vol. 132, pp. 15–22, 2015. DOI: 10.1016/j.proeng.2015.12.462.

[21] R. M. Christensen, "Mechanics of cellular and other low-density materials," *Int. J. Sol. Struct.*, vol. 37, no. 1–2, pp. 93–104, 2000. DOI: 10.1016/S0020-7683(99)00080-3.

[22] D. D. Luong, D. Pinisetty, and N. Gupta, "Compressive properties of closed-cell polyvinyl chloride foams at low and high strain rates: Experimental investigation and critical review of state of the art," *Compos. Part B: Eng.*, vol. 44, no. 1, pp. 403–416, 2013. DOI: 10.1016/j.compositesb.2012.04.060.

[23] S. Torquato, L. V. Gibiansky, M. J. Silva, and L. J. Gibson, "Effective mechanical and transport properties of cellular solids," *Int. J. Mech. Sci.*, vol. 40, no. 1, pp. 71–82, 1998. DOI: 10.1016/S0020-7403(97)00031-3.

[24] N. J. Mills, *Polymer Foams Handbook: Engineering and Biomechanics Applications and Design Guide*. New York: Elsevier, 2007.

[25] T. Gómez-del Río and J. Rodríguez, "Compression yielding of polypropylenes above glass transition temperature," *Eur. Polym. J.*, vol. 46, pp. 1244–1250, 2010. DOI: 10.1016/j.eurpolymj.2010.02.016.

[26] T. Ree and H. Eyring, "Viscosity, plasticity and diffusion as examples of absolute reaction rates," *J. Appl. Phys.*, vol. 26, pp. 793–800, 1955. DOI: 10.1063/1.1722098.

[27] D. Fotheringham and B. W. Cherry, "Comment on "The compression yield behaviour of polymethyl methacrylate over a wide range of temperatures and strain-rates," *J. Mater. Sci.*, vol. 11, pp. 1368–1370, 1976. DOI: 10.1007/BF00545162.

[28] T. Gómez-del Río, A. Salazar, and J. Rodríguez, "Effect of strain rate and temperature on tensile properties of ethylene–propylene block copolymers," *Mater. Des.*, vol. 42, pp. 301–307, 2012. DOI: 10.1016/j.matdes.2012.05.042.

[29] J. Richeton, S. Ahzi, L. Daridon, and Y. Rémond, "A formulation of the cooperative model for the yield stress of amorphous polymers for a wide range of strain rates and temperatures," *Polymer*, vol. 46, no. 16, pp. 6035–6043, 2005. DOI: 10.1016/j.polymer.2005.05.079.

[30] M. F. Ashby, "The properties of foams and lattices," *Philos. Trans. R. Soc. A.*, vol. 364, pp. 15–30, 2006. DOI: 10.1098/rsta.2005.1678.

[31] Y. Ma, X. Su, R. Pyrz, and J. Ch. Rauhe, "A novel theory of effective mechanical properties of closed-cell foam materials," *Acta Mech. Solida Sin.*, vol. 26, no. 6, pp. 559–569, 2013. DOI: 10.1016/S0894-9166(14)60001-X.

[32] T. Vu-Khank and M. El Majdoubi, "Entropy change with yielding and fracture of polypropylene," *Theor. Appl. Fract. Mech.*, vol. 51, pp. 111–116, 2009. DOI: 10.1016/j.tafmec.2009.04.002.

[33] J. Rault, "Yielding in amorphous and semi-crystalline polymers: The compensation law," *J. Non-Crystalline Solids*, vol. 235–237, pp. 737–741, 1998. DOI: 10.1016/S0022-3093(98)00667-X.